Preferential site distribution of dilute Pt and Ta in CoCr-based films: An extended x-ray absorption fine structure study

K. M. Kemner,[a] V. G. Harris, and W. T. Elam
U.S. Naval Research Laboratory, Washington, D.C. 20375

Y. C. Feng[b] and D. E. Laughlin
Department of Materials Science and Engineering, Carnegie Mellon University, Pittsburgh, Pennsylvania 15213

J. C. Woicik
National Institute of Standards and Technology, Gaithersburg, Maryland 20899

J. C. Lodder
MESA Research Institute, University of Twente, 7500 AE Enschede, The Netherlands

(Received 26 November 1996; accepted for publication 19 June 1997)

Extended x-ray absorption fine structure (EXAFS) measurements of $Co_{78}Cr_{22}$, $Co_{86}Cr_{12}Ta_2$, and $Co_{86}Cr_{12}Pt_2$ films were made to investigate the local structure and chemistry around Ta and Pt atoms to determine their site distributions in these alloys. Comparisons between the measured data and data collected from experimental standards and calculated using theoretical EXAFS simulation codes indicate that the Ta atoms are preferentially distributed to the Cr-enriched regions of the CoCr media, and the Pt atoms have an effect on the local environment of the Co atoms. Both Ta and Pt introduce a large amount of local structural disorder to the local environments in which they reside. The presence of Ta atoms in the Cr-enriched regions further reduces the magnetization of these regions, which enhances the magnetic isolation of the Co regions from each other. This helps improve the noise characteristics of the films. The portion of the Pt atoms residing in the Co-enriched regions increases the magnetic anisotropy of the films, thereby increasing their coercivity. © *1997 American Institute of Physics.* [S0021-8979(97)06018-0]

CoCr based alloy films are presently the mainstay magnetic recording media.[1–6] Numerous studies have shown that these films can be grown in ways to produce a compositional inhomogeneous microstructure having Co- and Cr-enriched regions (i.e., the number of Co–Co and Cr–Cr correlations are greater than what would be expected in the totally random situation).[3,7] This inhomogeneity plays an important role in determining the magnetic properties and recording characteristics of the films.[1–6,8–10] In recent years, the addition of Ta and Pt has been shown to enhance the recording properties of these media. Specifically, the addition of Ta has been shown to enhance the signal-to-noise characteristics of the CoCr longitudinal media.[4,11,12] This effect has been attributed to a reduction of the exchange-coupling between the neighboring magnetic grains, facilitated by a refinement of the microstructure[13] in the Co-enriched regions and a reduction in the magnetization of the intergranular Cr-enriched regions.[14] Alternatively, the use of Pt has been shown to increase the coercive force of CoCr films, thereby improving domain wall stability and the integrity of the written bit.[15] Although the role of Ta and Pt additives in improving the recording characteristics of CoCr media has been established empirically, no direct experimental evidence has been forthcoming to provide information as to the specific roles of these additives in modifying the microstructure of these media. To better understand their beneficial roles, one must determine first where the Ta and Pt atoms reside in this complex inhomogeneous material, and, secondly, how they affect the local environment at these sites.

In this article, we describe extended x-ray absorption fine structure (EXAFS) measurements and analysis of $Co_{78}Cr_{22}$, $Co_{86}Cr_{12}Ta_2$, and $Co_{86}Cr_{12}Pt_2$ thin films. By employing both qualitative ''fingerprinting'' and quantitative theoretical fitting analyses, we conclude that (1) the Ta atoms are preferentially distributed to the Cr-enriched regions in these films and have a direct effect on the average local environment of the Cr atoms and very little effect on the average local environment of the Co atoms and (2) the Pt atoms have an effect on the average local environment of the Co atoms. How the distribution of these large atoms provides the beneficial effects to the CoCr media, together with their effects on the local environment of Co and Cr, is discussed.

The 300-nm-thick magnetic films investigated in this study were rf sputtered onto 7059 Corning glass substrates in an LH Z-400 sputtering system. The target compositions were $Co_{78}Cr_{22}$, $Co_{86}Cr_{12}Ta_2$, and $Co_{86}Cr_{12}Pt_2$. The argon pressure during sputtering was 10 mTorr, and the forward power density was 2.5 W/cm^2. The initial substrate temperatures during film growth were ambient temperature and 260 °C. All films were capped with a 5 nm layer of Al to retard oxidation after removal from the deposition chamber.

X-ray absorption spectra at the Co K-, Cr K-, Ta L_{III}-, and Pt L_{II}-absorption edges were collected at room temperature via the total electron yield detection scheme,[16] using beam lines X23B and X23A2 at the National Synchrotron

[a]Current address: Argonne National Laboratory, Argonne, IL 60439. Electronic mail: ken_kemner@qmgate.anl.gov
[b]Current address: Headway Technologies Inc., 497 S. Hillview Drive, Milpitas, CA 95035.

 0021-8979/97/82(6)/2912/6/$10.00 © 1997 American Institute of Physics

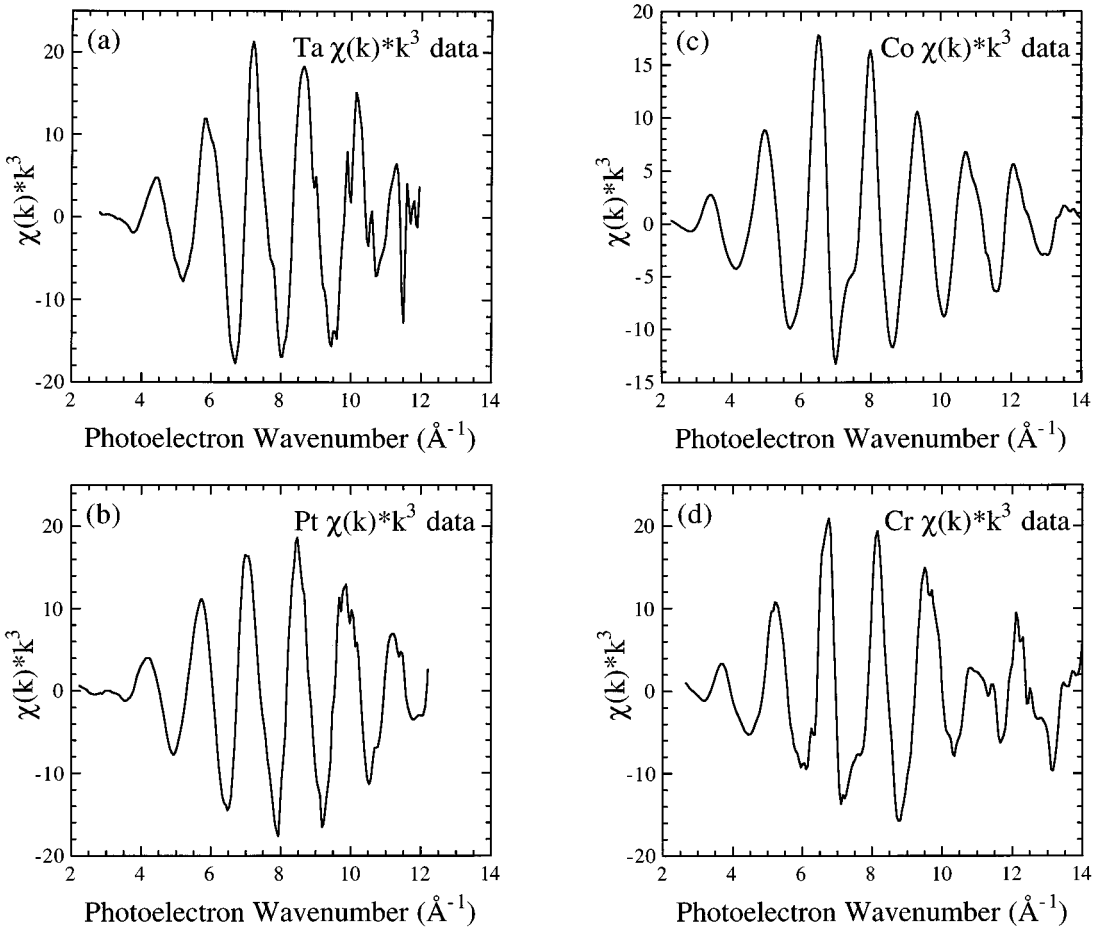

FIG. 1. (a)–(d) $\chi(k)*k^3$ data from CoCr(Ta or Pt) films depicting the quality of data analyzed in this work.

Light Source. The characteristics of the total electron yield detector used in these experiments have been described elsewhere.[17] The linearity of the experimental setup (at all absorption edges) was found to vary less than 0.1% for a 50% attenuation of the incoming x-ray beam.[17] Figures 1(a)–1(d) illustrates $\chi(k)$ (k^3-weighted) data representative of the quality of the data analyzed in this study. Because EXAFS provides average atomic information of the absorbing atoms, measurement of the Cr EXAFS for the $Co_{86}Cr_{12}Pt_2/Cr$ sample was not possible, since this film has a 100 Å Cr underlayer.[18]

The EXAFS data were subjected to established analysis procedures,[19] which included the normalization of the extended fine structure to the absorption edge step energy and height, removal of a nonoscillatory background curvature, conversion to photoelectron wave vector (k) space, and Fourier transformation to radial (r) coordinates. In this later form, the data can be interpreted similar to a radial distribution function where the centroid of the Fourier peak corresponds to the average bond distance (uncorrected for an electron phase shift) and where the amplitude and width of the peak corresponds to the coordination and atomic disorder of the atomic shells contributing to the peak. To obtain quantitative measurement of the average near-neighbor environment around each constituent, the nearest-neighbor Fourier peak, appearing near 2 Å, was Fourier-filtered to k-space and fitted using parametrized theoretical EXAFS spectra generated using the FEFF codes (version 3.1) of Rehr and co-workers.[20] The absorption edge energy shift, v_0, and the amplitude correction coefficient, S_0^2, which were used as inputs to these codes, were determined independently through a fitting analysis of data collected from Co, Cr, and Ta standards with simulated data. The analysis of the near-neighbor region allows the calculations of the average coordination number, radial distance, and Debye–Waller coefficient of atomic shells contributing to the local environment around the absorbing atoms. (The EXAFS Debye–Waller coefficient contains information on both the thermal and static displacement of atoms about an average radial distance.)

Figures 2(a) and 2(b) are plots of the Fourier transformed Ta and Pt EXAFS data (2.8–10.8 $Å^{-1}$ with 1.0 $Å^{-1}$ Hanning windows) for the CoCrTa and CoCrPt samples deposited at ambient (solid line) and 260 °C (dashed line) substrate temperatures. By comparing the profiles of these data to known structural standards having close-packed structures (e.g., Co, Cu, and Pt), one can conclude, for both substrate temperatures, that the Ta and Pt atoms reside in close-packed structures with a large amount of local disorder in the vicinity of the Ta and Pt atoms.[21] Analysis of the Fourier filtered near-neighbor peak[19] indicates that at least 95% of the local neighbors surrounding the Ta and Pt atoms are Co and/or Cr atoms.[22] Figure 3 shows the best fit to the Ta data from the

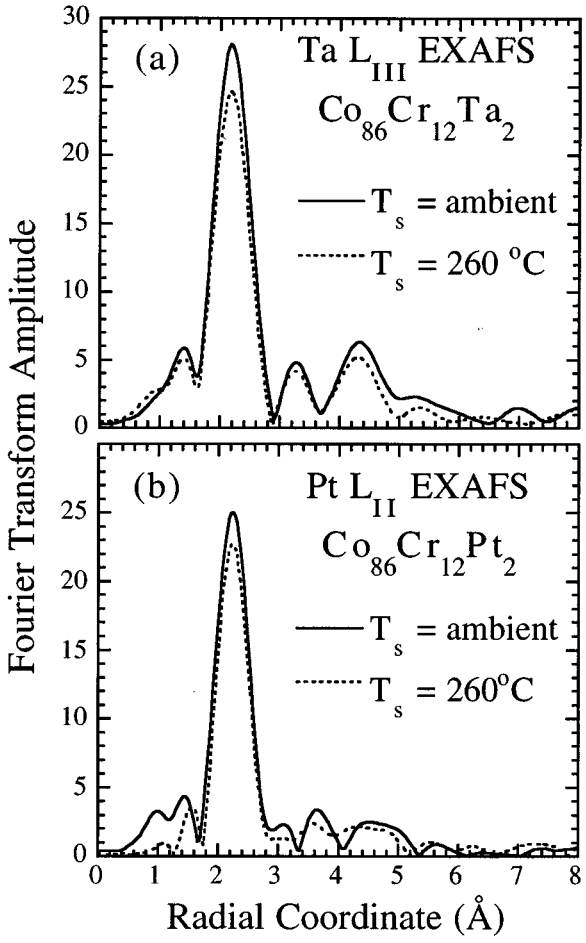

FIG. 2. (a) Fourier transformed Ta EXAFS data for the CoCrTa sample and (b) Fourier transformed Pt EXAFS data for the CoCrPt sample deposited at ambient and 260 °C substrate temperatures. (k ranges of 2.8–10.8 $Å^{-1}$, 1.0 $Å^{-1}$ Hanning window, with a k^3 weighing, were applied in the Fourier transformation.)

film deposited at ambient temperature (11.1±1.7 Co and/or Cr atoms at 2.55±0.02 Å).[23] These results do not indicate that any phase separation of the Ta or Pt atoms into clusters has taken place, as one might expect if the Ta or Pt atoms had phase separated from the CoCr phases. Further analysis of this region shows that for an increase in substrate deposition temperature, the average coordination of Ta and Pt decreases by 0.6±1.1 Co/Cr atoms, while the EXAFS Debye–Waller coefficient (structural disorder) increases by 0.001 ±0.004 $Å^2$.[22,23] These results are qualitatively evident by the reduction in the near-neighbor peak amplitude with increasing substrate temperature (see Fig. 2). This change in the EXAFS Debye–Waller coefficient indicates that the static displacement of atoms from a mean value increases with substrate deposition temperature. This trend is opposite to the increase in structural order that is typically observed when samples are thermally annealed or when deposition temperatures are increased. With increased substrate temperatures, the arriving adatoms have increased surface mobility, which allows for the selection of lower energy sites before the adatoms are ''frozen'' in place by the flux of arriving atoms. With this increased mobility, one expects a more ordered structure, one having fewer defects. The observed trend suggests that the Ta and Pt atoms act as sinks for lattice defects, consistent with their larger size relative to the Co and Cr atoms.

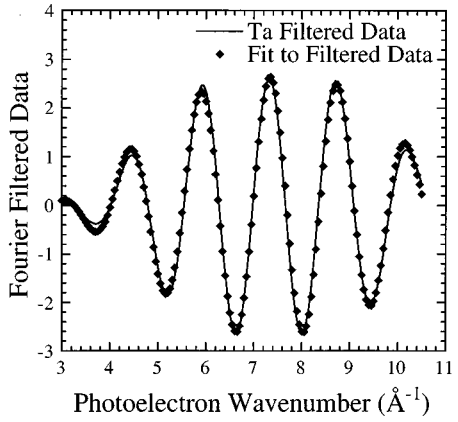

FIG. 3. Fit to Fourier filtered first shell Ta EXAFS data, showing that no clustering of the Ta atoms has occurred.

Because the samples studied here were grown at temperatures higher than the measurement temperature one may suspect that differential thermal expansion contributes to the observed disorder between samples. Harris and co-workers[24] have studied the effect of deposition temperature on the atomic disorder in vapor-quenched thin films in the temperature range that these samples were grown. Their findings show that, although this effect is measurable, it is much smaller than the disorder observed in the samples studied here. This leads us to conclude that the disorder in these samples cannot be solely attributable to atomic disorder or local strain fields arising from the differential thermal expansion.

Additionally, it is important to note that structural disorder is not always modeled well by a Gaussian distribution. When the width of a Fourier transformed peak is large (particularly if the static distribution of bondlengths is asymmetrical), the apparent number of neighbors may be low if modeled by a Gaussian distribution. To further investigate the observed decrease in coordination number with an increase in the initial substrate temperature, multishell fits to the Fourier filtered data were attempted to determine the magnitude of any asymmetrical distribution of bondlengths. Similar total coordination values and symmetrical bondlength distributions resulted from multishell fits of Co and/or Cr backscatterers to the Ta and Pt EXAFS data, thus indicating a negligible deviation from a symmetrical distribution.

Figure 4 shows the Co Fourier transformed EXAFS data (2.8–11.0 $Å^{-1}$ and 0.5 $Å^{-1}$ Hanning windows) for CoCrTa and CoCrPt samples deposited at ambient and 260 °C substrate temperatures. The Co data for the CoCr binary film is provided as a reference profile. With the addition of Ta and Pt, the Fourier peaks of the Co EXAFS data decrease relative to that of the data for the CoCr film, indicating an increase in disorder around the Co sites. Two qualitative observations in Fig. 4 are noteworthy. First, the reduction in amplitude of all of the Co Fourier peaks is much greater with the addition of Pt than is the case for Ta. Second, amplitude of the higher

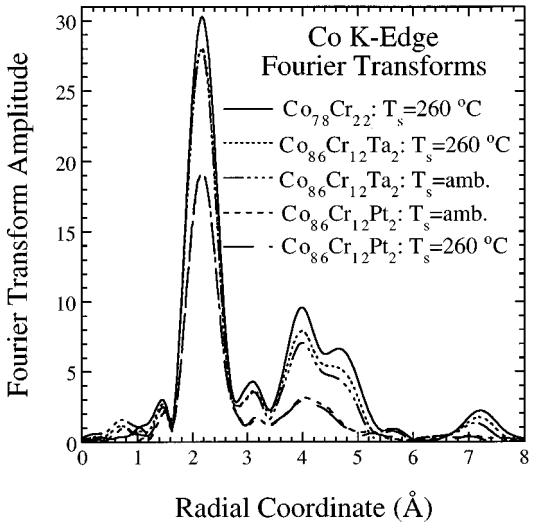

FIG. 4. Fourier transforms of Co EXAFS data for the CoCrTa and CoCrPt samples deposited at ambient and 260 °C substrate temperatures. Similar data collected from the CoCr film are presented as a reference profile. (k ranges of 2.8–11.0 Å^{-1}, 0.5 Å^{-1} Hanning window, with a k^3 weighing, were applied in the Fourier transformation.) Data are listed in order of decreasing amplitude.

order peaks in the Ta-containing alloys seems to increase with an increase in substrate deposition temperature (opposite to the trend observed in the Ta and Pt EXAFS results). The first observation indicates that the Co environment is more disordered by the addition of Pt than it is by the addition of Ta. The second observation indicates that the addition of the Ta causes very little increase in the structural disorder around Co. On the contrary, with an increasing substrate deposition temperature, an increase in structural order is observed in the higher coordination shells. This suggests that the Pt atoms are contributing a greater and more significant degree of strain to the local environment of the Co atoms, whereas the Ta atoms are not significantly affecting the local environment of the Co atoms.

Results of quantitative fitting of the Fourier filtered first shell Co K-edge data (1.2–3.4 Å and 0.5 Å Hanning window) from the CoCrTa and CoCrPt films deposited at ambient temperature (relative to the CoCr standard) are shown in Table I. Two different fitting scenarios are listed for each film: one where coordination number, radial distance, and EXAFS Debye–Waller factors were allowed to vary; and

TABLE I. Summary of EXAFS fitting analysis of the average local environments of Co atoms in CoCrTa and CoCrPt films deposited at ambient temperature.

Sample	Δr (Å)[a]	Coordination Number Change[a]	$\Delta\sigma^2$ (Å^2)[a]
CoCrTa	0.00±0.02	−1.6±2.0	−0.0004±0.001
CoCrTa[b]	0.00±0.02	0	0.0007±0.0005
CoCrPt	0.00±0.02	−3.0±2.0	0.0014±0.001
CoCrPt[b]	0.00±0.02	0	0.0038±0.0005

[a]All results are relative to the Fourier filtered shell data from a CoCr film.
[b]Results of fits when constraining the coordination number around Co in the CoCr standard and the CoCrTa and CoCrPt films to be equal.

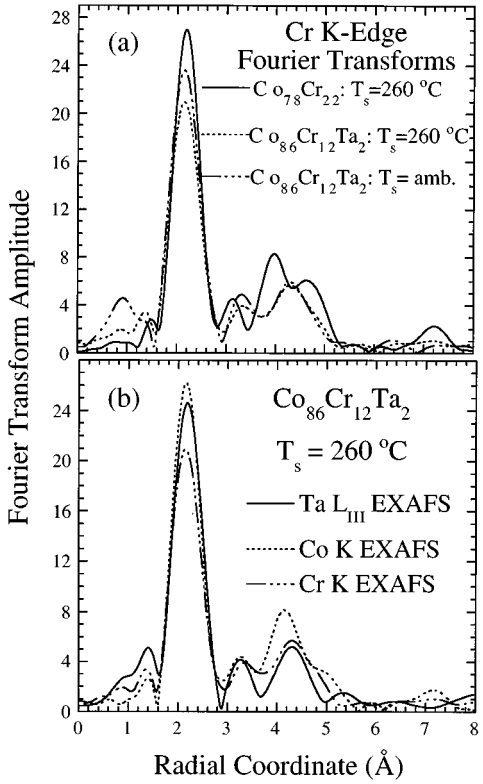

FIG. 5. (a) Fourier transformed Cr EXAFS data for CoCrTa deposited at ambient and 260 °C substrate temperatures. Similar data from the CoCr film are presented as a reference profile. (b) Fourier transformed Ta, Co, and Cr EXAFS data for the CoCrTa sample deposited at 260 °C. (k ranges of 3.0–12.0 Å^{-1}, 1.0 Å^{-1} Hanning window, with a k^3 weighing, were applied in the Fourier transformation.)

one where the coordination number was fixed to be 12 Co/Cr atoms (i.e., the same as the CoCr standard) and the radial distance and EXAFS Debye–Waller factor were allowed to vary.[23] Results of this fitting analysis indicate that with the addition of Ta, no discernible change occurs in bondlength, coordination number, or EXAFS Debye–Waller factor of the first shell atoms surrounding Co. The results in Table I do show, however, that the addition of Pt has a significant effect on the Co EXAFS Debye–Waller factor. This is strong evidence that the Pt atoms reside close to the Co atoms (i.e., the Co-enriched regions of the film), where they create significant structural disorder to the Co local environments. Because Cr edge measurements on the CoCrPt films were not possible, due to contamination from the Cr buffer layer, it is not possible to draw any conclusions concerning the effect of Pt on the local environment of the Cr atoms.[18] Finally, from these Co EXAFS results, there is no evidence that the Ta atoms play a role in directly affecting the local environment of the Co atoms.

If the addition of Pt results in an increased disorder of the higher coordination shells surrounding the Co atoms, these shells will no longer be resolved, and there should be a broadened low-amplitude peak between 3.5 and 5 Å. Our data show a low peak just above 4 Å.

Figure 5(a) is a plot of the Fourier transformed Cr EXAFS data for CoCr and CoCrTa films deposited at room temperature and 260 °C. Data collected from the CoCr bi-

nary film are presented as a reference profile. Qualitative inspection of the first Fourier peak shows a trend of reducing amplitude with increased substrate temperature. A similar trend was observed in the Ta EXAFS data of Fig. 2(a); however, as was illustrated in Fig. 4, no significant decrease in first shell amplitude was seen for the Co local environment in CoCrTa films. This definitively shows that the addition of Ta to CoCr thin films has a much greater effect on the Cr local environment than on the Co local environment. In addition, the higher order peak(s) (i.e., $3.0\ \text{Å} \leqslant r \leqslant 5.0\ \text{Å}$), seem to be highly disordered and/or shifted to higher radial distances. A similar trend was seen for the Co EXAFS data collected from the CoCrPt sample (see Fig. 4). Finally, in Fig. 5(b), where the Cr, Co, and Ta Fourier transformed EXAFS data for the CoCrTa sample are plotted together, an increase in disorder and/or a shift of the higher order Fourier peaks to higher radial distances is observed around the Cr and Ta atoms, but not around the Co atoms. Again, the Co EXAFS data for this sample are very similar to those of the CoCr sample (note Fig. 4). Taken together, these results are consistent with the Ta atoms preferentially residing in and increasing the disorder of the Cr-enriched regions of the film. Once again, the introduction of Ta is found to have little effect on the Co environment.

When dealing with vapor-quenched alloys, one often finds that temperature-composition structural trends set forth by equilibrium phase diagrams[25] are violated. This is not uncommon since the vapor-quenched structures often exist as metastable states. However, these diagrams can often provide insight into the structure and bonding arrangements even for alloys and mixtures existing in nonequilibrium states and for that reason they should be consulted.

Equilibrium phase diagrams of both Cr–Ta_1 and Co–Ta_2 indicate limited or no miscibility of Ta in the host element at room temperature. For the case of Cr–Ta, both high- and low-temperature phases of the Cr_2Ta intermetallic compound exist; the hexagonal MgZn_2-type ($C14$) structure at high temperature and the cubic MgCu_2-type ($C15$) structure at low temperature. About 4 at. % Ta is miscible in Cr at 1760 °C, but less than 1 at. % is miscible near 1250 °C and much less than 1 at. % is miscible at temperatures less than 1200 °C. Alternatively, several intermetallics form in the Co–Ta system, with the Co_2Ta phase being the most Co rich. However, miscibility of Ta in the Co host occurs only at temperatures greater than 422 °C where the maximum solubility is 4 at. % at a temperature of 1008 °C. From this information one cannot readily gain insight into the preferred bonding arrangements between Ta and Cr or Co.

Similarly, the Cr–Pt_3 system indicates limited solubility of Pt in the Cr host. Specifically, the Cr–Pt system is characterized by a broad homogeneous range of the Pt terminal solid solution and by the presence of three ordered intermediate phases (Cr_3Pt, CrPt, and CrPt_3). The solubility of Pt in Cr is 2.5 at. % at a temperature of 900 °C and reduces to approximately 1 at. % at temperatures less than 500 °C. In contrast, the Co–Pt_4 equilibrium diagram shows complete solubility of each element in the other. At temperatures greater than 422 °C the face centered cubic structure exists across the entire phase diagram, whereupon at lower temperatures the hexagonal close packed structure exists near the Co terminal (i.e., less than 20–30 at. % Pt). Ordered phases of CoPt and CoPt_3, having the AuCu ($L10$) and AuCu_3 ($L12$) structures, exists below temperatures of 825 and 750 °C, respectively. From this information one can expect Pt to have an affinity for close-packed bonding arrangements with Co, similar to our experimental results.

In summary, we have employed EXAFS measurements and analysis to show unambiguously that when small amounts of Ta are introduced to CoCr, they preferentially segregate to the Cr-enriched regions of the film. The addition of small amounts of Pt is shown to directly affect the local environment of the Co atoms. Because of the characteristics of the CoCrPt films (i.e., a Cr buffer layer), no measurements could be made to determine the effect of the addition of Pt on the local environment of the Cr atoms. The local environments of both Ta and Pt were found to have a large amount of local structural disorder. This effect is enhanced when the samples are grown at higher deposition temperatures. We interpret this counterintuitive trend to mean that these atoms act as sinks for lattice defects. In addition, both Ta and Pt atoms contribute significant local disorder, presumably through local strain fields, to the Co and Cr environments, respectively. The introduction of Ta has been shown to improve signal-to-noise performance. Rogers *et al.*[13] have shown that the addition of Ta results in a refinement of the CoCr microstructure, most notably a reduction in the length scale of the compositional separation. From the EXAFS analysis presented here, we now know that Ta resides preferentially in the Cr-enriched regions and that its introduction creates a significant local disorder in those regions. As was reported by Nakai *et al.*,[14] the additional of Ta leads to a reduced intragranular exchange coupling and to improved signal-to-noise characteristics. This improvement can be explained by the reduction in the magnetization of the Cr-enriched regions, which separate the Co-enriched grains, by the preferential distribution of Ta in those regions; an idea first put forth by Hwang *et al.*[26] On the other hand, the portion of Pt atoms which reside in the Co-enriched regions also creates local disorder, which in turn increases the local magnetocrystalline anisotropy, which causes an increase in the coercivity of the films. Enhanced coercive fields have been reported in Pt-containing CoCr alloys.[15]

ACKNOWLEDGMENTS

This research was performed in part at the National Synchrotron Light Source (Brookhaven National Laboratory, Upton, New York), which is sponsored by the U.S. Department of Energy. K. M. Kemner was supported by a National Research Council/Naval Research Laboratory Fellowship. The research carried out at Carnegie Mellon University was supported by Grant No. FG02-90-ER4523 from the U.S. Department of Energy. This research was also supported by the U.S. Department of Energy, Office of Energy Research, Office of Basic Energy Science and Office of Health and Environmental Research, under Contract No. W-31-109-Eng-38.

[1] C. W. Chen, J. Mater. Sci. **29**, 3125 (1991).
[2] S. Iwasaki and K. Ouchi, IEEE Trans. Magn. **14**, 849 (1978).

[3] J. C. Lodder, in *High Density Digital Recording*, NATO ASI Series, edited by K. H. J. Buschow, G. J. Long, and F. Grandjean (Kluwer, Dordrecht, 1995), Vol. 229, pp. 161–197.
[4] Y. Shen, D. E. Laughlin, and D. N. Lambeth, J. Appl. Phys. **76**, 8167 (1994).
[5] T. Yogi and T. A. Nguyen, IEEE Trans. Magn. **29**, 307 (1993).
[6] M. R. Kim, S. Guruswamy, and K. E. Johnson, IEEE Trans. Magn. **29**, 3673 (1993).
[7] K. M. Kemner, V. G. Harris, W. T. Elam, and C. J. Lodder, IEEE Trans. Magn. **30**, 4017 (1994).
[8] K. Yoshida, H. Kakibayashi, and H. Yasuoka, Mater. Res. Soc. Symp. Proc. **232**, 47 (1991).
[9] Y. Maeda and M. Takahashi, J. Appl. Phys. **68**, 4751 (1990).
[10] Y. Yahisa, K. Kimoto, K. Usamik, Y. Matsuda, J. Inagaki, K. Furusawa, and S. Narishige, IEEE Trans. Magn. **31**, 2836 (1995).
[11] T. Chen and T. Yamashita, IEEE Trans. Magn. **24**, 2700 (1988).
[12] T. Yogi, T. A. Nguyen, S. E. Lambert, G. L. Gorman, and G. Castillo, IEEE Trans. Magn. **26**, 1578 (1990).
[13] D. J. Rogers, Y. Maeda, and K. Takei, IEEE Trans. Magn. **30**, 3972 (1994)
[14] J. Nakai, E. Kusomoto, M. Kuwabara, T. Miyamot, M. R. Visokay, K. Yoshikawa, and E. Itayama, IEEE Trans. Magn. **30**, 3969 (1994).
[15] P. Glijier, J. Sivertsen, and J. Judy, J. Appl. Phys. **73**, 5563 (1993).
[16] A. Erbil, G. S. Cargill III, R. Frahm, and R. F. Boehme, Phys. Rev. B **37**, 2450 (1988).
[17] K. M. Kemner, J. Kropf, and B. A. Bunker, Rev. Sci. Instrum. **65**, 3667 (1994).
[18] It is important to note that these samples were not initially grown in order to perform Cr *K*-edge x-ray absorption experiments on them. A Cr buffer layer between the CoCrPt magnetic film and the Corning glass was used to provide a smoother film surface for earlier recording performance improvement studies.
[19] D. E. Sayers and B A. Bunker, in *X-ray Absorption: Principles, Applications, Techniques of EXAFS, SEXAFS and XANES*, edited by D. C. Koningsberger and R. Prins, (Wiley, New York, 1988), p. 211.
[20] J. J. Rehr, J. M. d. Leon, S. I. Zabinsky, and R. C. Albers, J. Am. Chem. Soc. **113**, 5135 (1991). The S_0^2 values used as inputs to simulate the Co and Cr XAFS data were 0.85, and the value of the inputs used to simulate the Pt and Ta XAFS data were 0.80.
[21] For a detailed discussion of the qualitative features of Fourier transformed EXAFS data that are indicative of body center cubic (bcc), face center cubic (fcc), and hexagonal close-packed (hcp) structures, see: K. M. Kemner, W. T. Elam, V. G. Harris, Y. U. Idzerda, and J. A. Wolf, J. Vac. Sci. Technol. B **14**, 3207 (1996).
[22] K. M. Kemner, V. G. Harris, W. T. Elam, Y. C. Feng, D. E. Laughlin, and J. C. Woicik, IEEE Trans. Magn. **31**, 2806 (1995).
[23] The magnitude of the error bars quoted here represents a doubling of the residual (i.e., χ^2) relative to its value for the best fit of the experimental data. For further details concerning fits to the Ta edge data, see Ref. 22.
[24] V. G. Harris, W. T. Elam, N. C. Koon, and F. Hellman, Phys. Rev. B **49**, 3637 (1994).
[25] *Binary Alloy Phase Diagrams Vol. II*, edited by T. B. Massalski (ASM International, 1990), pp. 1225, 1226, 1244, 1245, 1313–1316, 1338–1340.
[26] C. H. Hwang, Y. S. Park, P. W. Jang, and T. D. Lee, IEEE Trans. Magn. **29**, 3733 (1993).